SvedbergOpen
DISSEMINATION OF KNOWLEDGE

International Journal of Artificial Intelligence and Machine Learning

Publisher's Home Page: https://www.svedbergopen.com/

Research Paper Open Access

Optimal Load Frequency Control of Two-Area Power System using Sailfish Optimization Algorithm

Tarun Gupta[1], D. K. Sambariya[2]

[1]Department of Electrical Engineering Rajasthan Technical University Kota, India. E-mail: tarun92gupta@live.com
[2]Department of Electrical Engineering Rajasthan Technical University Kota, India. E-mail: dksambariya@rtu.ac.in

Abstract
In this paper, the load frequency control of two-area interconnected hydro-thermal power system is presented. The proportional-integral-derivative (PID) controller gain parameters are optimized using sailfish Optimization (SFO) algorithm for best optimal solution. The integral square error (ISE) function is used as objective function. The study of load frequency control of the hydro-thermal interconnected power system is presented and compared based on the performance indices and step response specifications. The behavior of the interconnected system is compared based on tie-line power and change in frequency in both the areas.

Keyword: Load Frequency Control (LFC), Sailfish Optimization (SFO) Algorithm, Proportional-Integral-Derivative (PID) Controller, Integral Square Error (ISE)

INTRODUCTION

The stability of power system is essential to ensure the efficient operation and reliable electricity supply to the consumers. The reliability and stability of power system is depend on its frequency deviation from the pre-defined values [1]. The system imbalance is caused by the difference between demand and generation. To keep an interconnected power system stable, the load frequency control (LFC) technique is employed[2]. In recent years, the development of LFC presented by different authors using different controllers with the help of different optimisation techniques and with the different objective function. Singh et al. [3] presented the PID control of reheat turbine using teaching learning based optimization. Liu et al. [4] presented the multi area LFC using event triggered optimization technique. Feleke et al. [5], presented the deferential evolution (DE) and particle swarm optimisation (PSO) tuning of PID controller. Fagna et al. [6] presented the LFC of the single area reheat thermal power system using EHO. Goswami and Shatil [7], presented the LFC system analysis using genetic algorithm (GA), adaptive neuro-fuzzy interface system (ANFIS) and PSO tuned PID controller. Dash et al. [8] presented the LTSM+GA-PID controller for two-area power system. Sree Vidya et al. [9], presented the different classical methods of PID controller tuning for automatic LFC system. Yogi [10, 11] presented IoT and ML methods for real time fault detection in the electrical system. Iqbal et al. [12] presented the hybrid optimization algorithm for tuning of PID controller for two-area power system.
The stability of interconnected power systems is a critical factor in modern energy management. Load Frequency Control (LFC) plays a key role in maintaining system stability by ensuring that frequency deviations are minimized following load perturbations [13]. Traditional PID controllers have been widely used in LFC; however, their performance depends heavily on optimal parameter tuning [14]. To address this challenge, different optimization techniques have been studied. This study emphases on the Sailfish Optimization (SFO) algorithm for PID tuning, demonstrating its superiority over ABC-PID.
The structure of this paper as follows: Section II describe the two-area power system under study with the formulation of controller. Section III describe a brief description of optimisation algorithm. The results of the system performance is presented in the Section IV and followed by the conclusion of the presented work in Section V.

PROBLEM FORMULATION

A. Two-area Power System

A linear two-area Hydro-thermal power system with two control areas of 2000 MW and 50 Hz is shown in Figure 1 as presented in [12]. The two-area power system is integrated and comprises a thermal power system with reheat turbine in area-1 and a hydropower system in area-2 [15].

1) Thermal Power System: The area-1 of given power system in Fig. 1 represents the thermal power system with reheat turbine and the component description as follows:

The governor transfer function is given by Eq. 1.

$$G_{sg}(s) = \frac{1}{1+sT_g} \qquad (1)$$

The steam turbine transfer function is given by Eq. 2.

$$G_{st}(s) = \frac{1}{1+sT_t} \qquad (2)$$

The reheater transfer function is given by Eq. 3.

$$G_r(s) = \frac{1+sK_rT_r}{1+sT_r} \qquad (3)$$

Where, T_g is steam governor time constant, T_t is steam turbine time constant, T_r is reheater time constant and K_r is reheater coefficient.

2) Hydro Power System: The area-2 of the presented interconnected power system signifies the hydro power system in Figure 1 and the component description as follows:

The hydro governor transfer function is given by Eq. 4.

$$G_{hg}(s) = \frac{1}{1+sT_{hg}} \qquad (4)$$

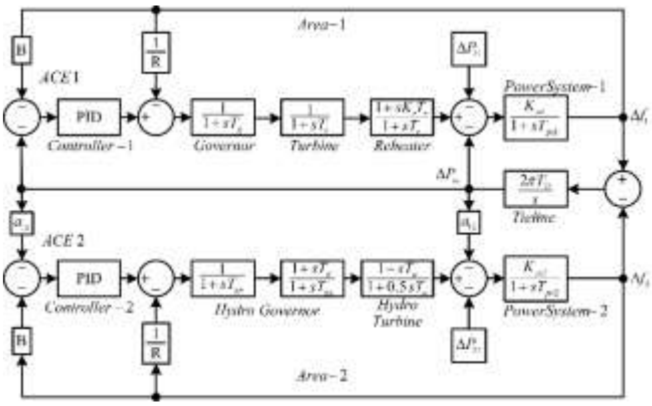

Fig. 1.Two-area hydro-thermal Interconnected power system model representation.

$$G_{hd}(s) = \frac{1+sT_R}{1+sT_{Rh}} \qquad (5)$$

Eq. 5 represents the droop compensation for hydro governor. The hydro turbine transfer function is given by Eq. 6.

$$G_{ht}(s) = \frac{1-sT_w}{1+0.5sT_w} \qquad (6)$$

Where, T_{hg} is time constant of hydro-governor, T_R is reset time of hydro turbine speed governor, T_{Rh} is transient droop time constant and T_w is penstock water time constant. The power system transfer function is given by Eq. 7 which is the core part of the load frequency control in the interconnected system.

$$G_{ps}(s) = \frac{K_{ps}}{1+sT_{ps}} \qquad (7)$$

Where, K_{ps} is gain constant of power system and T_{ps} is time constant of power system.

Both areas of the interconnected system is connected through tie-line. The tie-line block is given by $2\pi T_{12}/s$ where, T_{12} represents the tie-line coefficient.

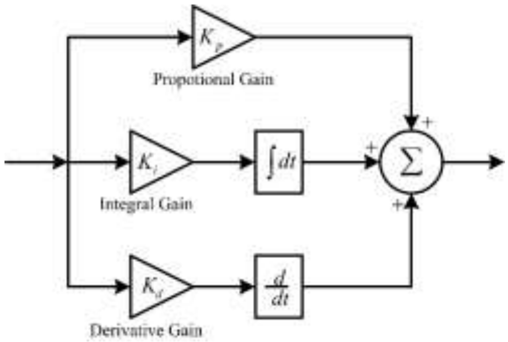

Fig. 2.PID controller block representation

B. PID Controller

The proportional-integral-derivative (PID) controller is used to control the frequency deviation in the area-1 and area-2 of the given interconnected power system [16]. The general structure of PID controller is shown in Fig. 2.

The PID controller transfer function equation is shown in Eq. 8.

$$G_c(s) = K_p + \frac{K_i}{s} + K_d s \qquad (8)$$

Where, K_p, K_i and K_d are the proportional, integral and derivative gains, respectively.

Methodology

This section describes a swarm-based sailfish optimisation algorithm that draws inspiration from nature. The behaviour of sailfish in the search space describes the Sailfish Optimisation (SFO) algorithm. Two types of populations are included in the search space by this nature-inspired algorithm: the sailfish population and the sardine population. [17]. The best solution and diversification in the search space are attributed to the populations of sailfish and sardines, respectively..

C. Sailfish Optimisation Algorithm

1. Initialization: In the SFO algorithm, the position of sailfish is assumed as variable of the problem and sailfish are candidate solutions in the search space. The population over the solution space is randomly generated. The sailfish position (SF_p) is given by Eq. 9 as presented in [17].

$$SF_p = \begin{bmatrix} SF_{1,1} & SF_{1,2} & \cdots & SF_{1,d} \\ SF_{2,1} & SF_{2,2} & \cdots & SF_{2,d} \\ \vdots & \vdots & \vdots & \vdots \\ SF_{m,1} & SF_{m,2} & \cdots & SF_{m,d} \end{bmatrix} \qquad (9)$$

Each sailfish's fitness is determined by calculating the fitness function using Eq. 10:

$$Fitness\ value\ of\ sailfish = f(sailfish) = f(SF_1, SF_2, ..., SF_m) \qquad (10)$$

The fitness value of each sailfish (SF_F) is shown by Eq. 11:

$$SF_F = \begin{bmatrix} f\left(SF_{1,1} & SF_{1,2} & \cdots & SF_{1,d}\right) \\ f\left(SF_{2,1} & SF_{2,2} & \cdots & SF_{2,d}\right) \\ \vdots & \vdots & \vdots & \vdots \\ f\left(SF_{m,1} & SF_{m,2} & \cdots & SF_{m,d}\right) \end{bmatrix} = \begin{bmatrix} F_{SF_1} \\ F_{SF_2} \\ \vdots \\ F_{SF_m} \end{bmatrix} \qquad (11)$$

The group of sardines that are swimming in the search space is taken into consideration by the SFO algorithm. Thus, sardines (S_p) position and fitness values are as follows:

$$S_p = \begin{bmatrix} S_{1,1} & S_{1,2} & \cdots & S_{1,d} \\ S_{2,1} & S_{2,2} & \cdots & S_{2,d} \\ \vdots & \vdots & \vdots & \vdots \\ S_{n,1} & S_{n,2} & \cdots & S_{n,d} \end{bmatrix} \qquad (12)$$

$$S_F = \begin{bmatrix} f(S_{1,1} & S_{1,2} & \cdots & S_{1,d}) \\ f(S_{2,1} & S_{2,2} & \cdots & S_{2,d}) \\ \vdots & \vdots & \vdots & \vdots \\ f(S_{m,1} & S_{m,2} & \cdots & S_{m,d}) \end{bmatrix} = \begin{bmatrix} F_{S_1} \\ F_{S_2} \\ \vdots \\ F_{S_m} \end{bmatrix} \quad (13)$$

where f is the objective function and (S_F) saves the fitness value of each sardine.

Sardines and sailfish are corresponding factors in this method that determines the optimal solution. Sardines are in charge of determining the ideal location inside the search space, whereas sailfish are in charge of the optimum search area. When looking for the best spot, the sailfish updates its location and hunts the sardines.

2. Elitism: The good solution can be lost while updating the position of the search space and new positions may be lower than the old position. To overcome this, an elitism selection is employed. Elitism retains the old best solution into next generation. In every iteration, the sailfish with the best position is regarded as an elite. The best target is thought to be an injured sardine, and the fittest remedy is an exceptional sailfish. $X^i_{e\_SF}$ is the position of the injured sardine and $X^i_{i\_S}$ is the positions of the elite sailfish with the best fitness at i^{th} iteration.

3. Attack-alternation approach: The attack strategy of shows the behaviour of sailfish attacking the pray school. The positions of the sardines and sailfish shift throughout the attack phase. The location of the hunted sardine is eliminated, and the positions of the sailfish are altered by the arrival of fresh sailfish. At the i^{th} iteration of the SFO algorithm, sailfish X^i_{SFnew} new position updates as follows:

$$X^i_{SFnew} = X^i_{e\_SF} - \lambda_i \times \left(rand(0,1) \times \left(\frac{X^i_{e\_SF} + X^i_{i\_S}}{2} \right) - X^i_{SFold} \right) \quad (14)$$

Where, λ_i is a coefficient at the i^{th} iteration represented by Eq. 15:

$$\lambda_i = 2 \times rand(0,1) \times PD - PD \quad (15)$$

Where, the number of prey during each iteration is indicated by the prey density (PD) as shown in Eq. 16.

$$PD = 1 - \left(\frac{N_{SF}}{N_{SF} + N_S} \right) \quad (16)$$

Where, N_{SF} and N_S represents the number of sailfish and number of sardines respectively. N_{SF} is defined by $N_S \times PP$ where, PP represents the percentage of sardine population.

4. Hunting and capturing prey: The new location of sardine X^i_{Snew} during the i^{th} iteration of the SFO algorithm may be provided as:

$$X^i_{Snew} = r \times \left(X^i_{SFelite} - X^i_{S_{old}} + AP \right) \quad (17)$$

where $X^i_{SFelite}$ represents best position of elite sailfish, $X^i_{S_{old}}$ represents old position of sardine, r is a random number between 0 and 1 and Attack Power of sailfish (AP) at each iteration is given by:

$$AP = A \times \left(1 - \left(2 \times Itr \times \varepsilon\right)\right) \quad (18)$$

Where, A and ε are notations for reducing the value of power attack linearly from A to 0. Using AP parameter, the update position of sardines (α) and the number of variables of them (β) can be calculated as follows:

$$\alpha = N_S \times AP \quad (19)$$

$$\beta = d_i \times AP \quad (20)$$

where, d_i represents the number of variables at i^{th} iteration and N_S represents the number of sardines for each cycle in algorithm. To increase the likelihood of hunting new prey, the sailfish's position replaces the most recent location of the hunted sardine. The following equation is suggested:

$$X^i_{SF} = X^i_s \quad if \quad f(S_i) < (SF_i) \quad (21)$$

where, X^i_S represents the current location of sardine at i^{th} iteration and X^i_{SF} represents the current location of sailfish at i^{th} iteration. Table I shows the pseudocode for the SFO algorithm.

TABLE I. PSEUDOCODE OF SAILFISH OPTIMIZATION ALGORITHM

Set the sailfish and sardine populations at random. Set parameters $(A = 4,\ \varepsilon = 0.001)$. Calculate the fitness value of sailfish and sardines.

```
Find the best values and assume that they are an elite
sailfish and injured sardine respectively.
  while the termination conditions are not satisfied
    for every sailfish
      Calculate λ_i using Eq. 15
      Calculate the sailfish's position using Eq. 14
    end for
 Calculate Attack Power using Eq. 18
      if Attack Power < 0.5
        Calculate α using Eq. 19
        Calculate β using Eq. 20
        Based on the values of α and β, choose a set
of sardines.
   Using Eq. 17, update the position of sardines.
      else
        Using Eq. 17, update the position of sardines.
      end if
    Determine each sardine's fitness.
  If the population of sardines has a better
solution Use Eq. 13 to replace a sailfish for a
wounded sardine.
   Eliminate the hunted sardine from population.
          Update the best sailfish and best sardine
end if
  end while
Return best sailfish
```

TABLE II. PID CONTROLLER GAINS OBTAINED USING SFO AND CONTROLLER GAINS IN LITERATURE.

Controller	Area	K_p	K_i	K_d
ABC-PID [12]	1	2	0.3878	0.0679
	2	0.0433	1.1317	1.62589
Proposed (SFO-PID)	1	1.9875	1.9865	0.9987
	2	0.9945	0.1345	0.7166

D. Objective Function

The tuning of PID controller gains are considered as an optimisation problem. To minimise the error signal in the system response the integral square error (ISE) function is used [18] and is represented by Eq. 16.

$$ISE = \int_0^{\infty} \left(|\Delta f_1|^2 + |\Delta f_2|^2 + |\Delta P_{tie}|^2 \right) dt \qquad (16)$$

RESULT AND DISCUSSION

The simulation of two-area interconnected system is perform using MATLAB/Simulink software version 2018a represented in this section. During the course of simulation the controller gain parameters are tuned using SFO algorithm. The PID controller gain parameters K_p, K_i and K_d tuned using SFO algorithm of Area-1 and Area-2 are shown in Table II. The simulation is done with the consideration of 1% step load perturbation in area-1.

The value of controller gains K_p, K_i and K_d for area-1 is 1.9875, 1.9865 and 0.9987 respectively. The step response specifications for area-1 is shown in Table III and compared with the Iqbal, 2024 [12] in literature. Fig. 1 shows the response comparison of change in frequency (Δf_1) in area-1 with the ABC-PID in literature. Table IV represents the performance indices comparison with the data in literature.

The PID controller gains of for area-2 K_p, K_i and K_d are 0.9945, 0.1345 and 0.7166 respectively. The step response specification of area-2 is shown in Table V. Fig. 2 represents the change in frequency (Δf_2) in area-2 with comparing the data in literature. The comparison of performance indices for change in frequency shown in Table VI.

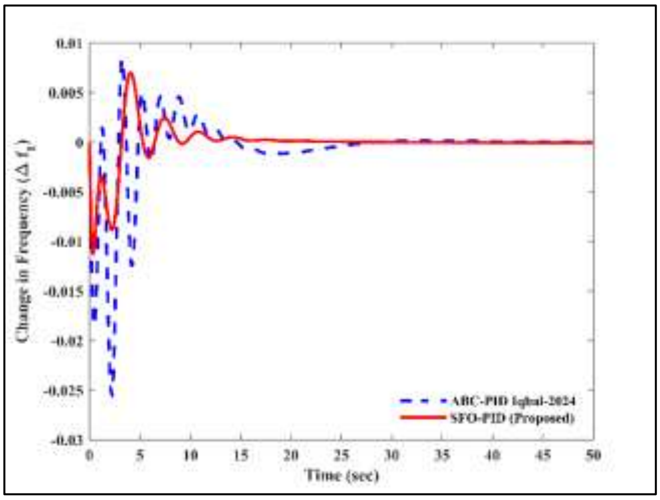

Fig. 3.Comparision of change in frequency response in area-1 using proposed SFO-PID and ABC-PID.

TABLE III. STEP RESPONSE SPECIFICATIONS FOR CHANGE IN FREQUENCY IN AREA-1

Controller	Rise Time	Settling Time	Peak Time	Overshoot
ABC-PID [12]	1.46×10^{-7}	23.9944	2.2	2.46×10^{8}
SFO-PID (Proposed)	2.33×10^{-4}	17.9193	0.3	1.77×10^{5}

TABLE IV. PERFORMANCE INDICES FOR CHANGE IN FREQUENCY IN AREA-1

Controller	ITAE	IAE	ISE	ITSE
ABC-PID [12]	0.5084	0.0772	7.90×10^{-4}	0.0021
SFO-PID (Proposed)	0.2415	0.0391	2.05×10^{-4}	4.82×10^{-4}

The comparison of change in tie-line power (ΔP_{tie}) for proposed method with the data in literature and step response specification is shown in Table VI and graphically represents in Fig. 3. The performance indices of using proposed method is compared in Table VII. Thus LFC of interconnected power system using SFO algorithm is compared with the literature ABC-PID [12]. The comparison of the proposed SFO-PID method with the ABC-PID in literature shows the better response based on the step response specification and performance indices for the interconnected hydro-thermal system.

TABLE V. STEP RESPONSE SPECIFICATIONS FOR CHANGE IN FREQUENCY IN AREA-2

Controller	Rise Time	Settling Time	Peak Time	Overshoot
ABC-PID [12]	1.10×10^{-7}	23.5073	1.5	1.05×10^{8}
SFO-PID (Proposed)	1.79×10^{-4}	14.5975	1.6	2.04×10^{5}

TABLE VI. PERFORMANCE INDICES FOR CHANGE IN FREQUENCY IN AREA-2

Controller	ITAE	IAE	ISE	ITSE
ABC-PID [12]	0.4622	0.0641	6.35×10^{-4}	0.0015
SFO-PID (Proposed)	0.2481	0.0427	3.14×10^{-4}	7.15×10^{-4}

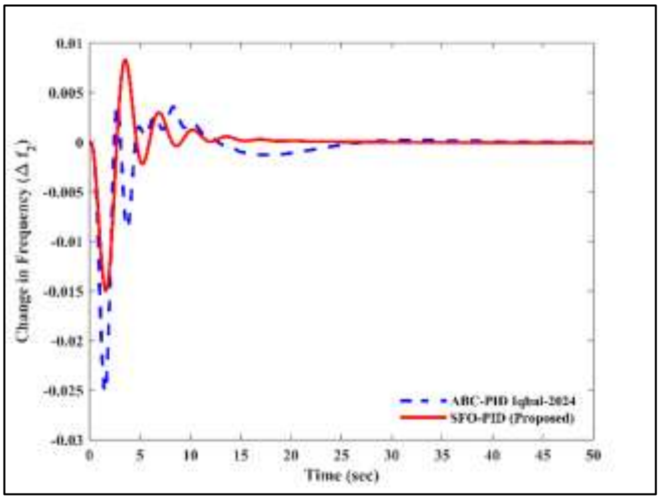

Fig. 4.Comparision of change in frequency response in area-2 using proposed SFO-PID and ABC-PID.

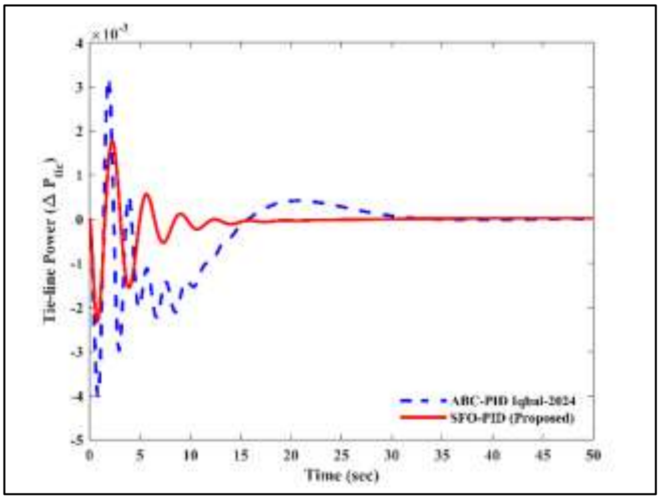

Fig. 5.Comparision of change in tie-line power of interconnected power system.

TABLE VII. STEP RESPONSE SPECIFICATIONS FOR CHANGE IN TIE-LINE POWER FOR TWO-AREA POWER SYSTEM

Controller	Rise Time	Settling Time	Peak Time	Overshoot
ABC-PID [12]	7.91×10^{-10}	29.836	0.8	3.06×10^{-10}
SFO-PID (Proposed)	0.001	18.1772	0.8	1.36×10^{-5}

TABLE VIII. PERFORMANCE INDICES FOR CHANGE IN TIE-LINE POWER FOR TWO-AREA POWER SYSTEM

Controller	ITAE	IAE	ISE	ITSE
ABC-PID [12]	0.2256	0.0253	4.18×10^{-5}	2.27×10^{-4}
SFO-PID (Proposed)	0.0695	0.0083	8.64×10^{-6}	2.14×10^{-5}

CONCLUSION

The analysis of the two-area interconnected hydro-thermal power system with the Sailfish Optimisation Algorithm tuned PID controller is discussed. When compared to ABC-PID in the literature, it is shown that the suggested approach exhibits the best reaction and performance based on load frequency control in power systems. The proposed approach effectively minimizes frequency deviations, reduces settling time, and improves overall system performance. Future work will focus on real-time implementation and testing under various load disturbances.

REFERENCES

[1] P. Kundur, Power system stability (Power system stability and control, no. 2). 2007.

[2] H. Saadat, Power System Analysis. PSA Publishing, 2009.

[3] A. Singh, S. Yadav, N. Tiwari, D. K. Nishad, and S. Khalid, "Optimized PID controller and model order reduction of reheated turbine for load frequency control using teaching learning-based optimization," Scientific Reports, vol. 15, no. 1, p. 3759, 2025/01/30 2025, doi: 10.1038/s41598-025-87866-z.

[4] Y. Liu, Z. Yuan, D. Xu, X. Xie, and J. H. Park, "Adaptive Event-Triggered Load Frequency Control for Multi-Area Power Systems Against Mixed Cyber-Attacks," IEEE Transactions on Smart Grid, vol. 16, no. 2, pp. 1732–1743, 2025, doi: 10.1109/TSG.2024.3492995.

[5] S. Feleke, R. Satish, S. R. Salkuti, and A. Y. Abdelaziz, "Load Frequency Control in Two-Area Interconnected Systems Using DE-PID and PSO-PID," in Power Quality in Microgrids: Issues, Challenges and Mitigation Techniques, S. R. Salkuti, P. Ray, and A. R. Singh Eds. Singapore: Springer Nature Singapore, 2023, pp. 391–407.

[6] D. K. Sambariya and R. Fagna, "A novel Elephant Herding Optimization based PID controller design for Load frequency control in power system," in 2017 International Conference on Computer, Communications and Electronics (Comptelix), 1–2 July 2017 2017, pp. 595–600, doi: 10.1109/comptelix.2017.8004039. [Online]. Available: http://dx.doi.org/10.1109/comptelix.2017.8004039

[7] N. Goswami and A. H. M. Shatil, "Performance Analysis of Load Frequency Control for Power Plants Using Different Optimization Techniques," in 2023 3rd International Conference on Robotics, Electrical and Signal Processing Techniques (ICREST), 7–8 Jan. 2023 2023, pp. 138–142, doi: 10.1109/ICREST57604.2023.10070029.

[8] R. Dash, K. J. Reddy, B. Mohapatra, M. Bajaj, and I. Zaitsev, "An approach for load frequency control enhancement in two-area hydro-wind power systems using LSTM + GA-PID controller with augmented lagrangian methods," Scientific Reports, vol. 15, no. 1, p. 1307, 2025/01/08 2025, doi: 10.1038/s41598-025-85639-2.

[9] A. Sree Vidya, V. Bharath Kumar, Y. V. Pavan Kumar, D. John Pradeep, and C. Pradeep Reddy, "Design of Automatic Load Frequency Control Loop Using Classical PID Control Methods," in Control Applications in Modern Power Systems, Singapore, J. Kumar, M. Tripathy, and P. Jena, Eds., 2023: Springer Nature Singapore, in Control Applications in Modern Power Systems, pp. 153–176.

[10] T. Yogi, "REAL-TIME FAULT DETECTION AND DIAGNOSIS OF SOLAR PHOTOVOLTAIC SYSTEMS FOR RAILWAY MICROGRID USING IOT AND MACHINE LEARNING," International Journal of Applied Mathematics, vol. 38, no. 11s, pp. 1169–1184, 2025.

[11] V. Singh, S. Ali, T. Yogi, D. Birla, and A. S. Naruka, "Minimizing THD in Railway's HOG using MLI in Hybrid Distributed Generation System," ed: Jul, 2025.

[12] M. S. Iqbal, M. F. A. Limon, M. M. Kabir, M. K. M. Rabby, M. J. A. Soeb, and M. F. Jubayer, "A hybrid optimization algorithm for improving load frequency control in interconnected power systems," Expert Systems with Applications, vol. 249, p. 123702, 2024/09/01/ 2024, doi: https://doi.org/10.1016/j.eswa.2024.123702.

[13] S. K. Pandey, S. R. Mohanty, and N. Kishor, "A literature survey on load–frequency control for conventional and distribution generation power systems," Renewable and Sustainable Energy Reviews, vol. 25, pp. 318–334, 2013/09/01/ 2013, doi: https://doi.org/10.1016/j.rser.2013.04.029.

[14] Y. V. Hote and S. Jain, "PID controller design for load frequency control: Past, Present and future challenges," IFAC-PapersOnLine, vol. 51, no. 4, pp. 604–609, 2018/01/01/ 2018, doi: https://doi.org/10.1016/j.ifacol.2018.06.162.

[15] I. C. Report, "Dynamic Models for Steam and Hydro Turbines in Power System Studies," IEEE Transactions on Power Apparatus and Systems, vol. PAS-92, no. 6, pp. 1904–1915, 1973, doi: 10.1109/TPAS.1973.293570.

[16] S. Shadravan, H. R. Naji, and V. K. Bardsiri, "The Sailfish Optimizer: A novel nature-inspired metaheuristic algorithm for solving constrained engineering optimization problems," Engineering Applications of Artificial Intelligence, vol. 80, pp. 20–34, 2019/04/01/ 2019, doi: https://doi.org/10.1016/j.engappai.2019.01.001.

[17] R. R. Shukla, M. M. Garg, A. K. Panda, and D. Das, "Enhancing load frequency control with plug-in electric vehicle integration in non-reheat thermal power systems," Electrical Engineering, vol. 106, no. 3, pp. 3305–3320, 2024/06/01 2024, doi: 10.1007/s00202-023-02144-3.